The EMBO Journal (2010) 29, 855–867 | © 2010 European Molecular Biology Organization | Some Rights Reserved 0261-4189/10
www.embojournal.org

THE EMBO JOURNAL

EMBO open

Evidence for a protein tether involved in somatic touch

Jing Hu[1,3,4,*], Li-Yang Chiang[1,3], Manuel Koch[2] and Gary R Lewin[1,*]

[1]Department of Neuroscience, Max-Delbrück Center for Molecular Medicine and Charité Universitätsmedizin Berlin, Berlin-Buch, Germany and [2]Center for Biochemistry, Department of Dermatology, and Center for Molecular Medicine Cologne, Medical Faculty, University of Cologne, Cologne, Germany

The gating of ion channels by mechanical force underlies the sense of touch and pain. The mode of gating of mechanosensitive ion channels in vertebrate touch receptors is unknown. Here we show that the presence of a protein link is necessary for the gating of mechanosensitive currents in all low-threshold mechanoreceptors and some nociceptors of the dorsal root ganglia (DRG). Using TEM, we demonstrate that a protein filament with of length ~100 nm is synthesized by sensory neurons and may link mechanosensitive ion channels in sensory neurons to the extracellular matrix. Brief treatment of sensory neurons with non-specific and site-specific endopeptidases destroys the protein tether and abolishes mechanosensitive currents in sensory neurons without affecting electrical excitability. Protease-sensitive tethers are also required for touch-receptor function *in vivo*. Thus, unlike the majority of nociceptors, cutaneous mechanoreceptors require a distinct protein tether to transduce mechanical stimuli.

The EMBO Journal (2010) **29,** 855–867. doi:10.1038/emboj.2009.398; Published online 14 January 2010
Subject Categories: signal transduction; neuroscience
Keywords: extracellular matrix; ion channels; laminin; mechanotransduction; proteases

Introduction

Different classes of ion channel proteins can be opened by ligands, voltage or temperature (Fain, 2003). A fourth class of ion channels can be opened by mechanical force and such mechanosensitive channels are thought to underlie mechanoelectric transduction in sensory cells (Gillespie and Walker, 2001; Hu *et al*, 2006; Wetzel *et al*, 2007). Essentially two models of gating have been proposed for sensory mechanosensitive channels. In the first model, force changes within the lipid bilayer act directly on the channel protein to facilitate opening and this model has been largely proven for bacterial mechanosensitive channels like MscL and MscS (mechanosensitive channels of large or small unitary conductance) (Sukharev *et al*, 1993, 1994; Kung, 2005). Members of another class of mammalian potassium channels belonging to the two pore potassium channel family have also been shown to be gated by force changes in the lipid bilayer (Honore, 2007). In the second model, protein tethers are proposed to transfer force from the surrounding matrix to the ion channel to promote opening (Chalfie, 2009). The tether model is well-supported for hair cells of the inner ear where a protein filament called the tip link, thought to consist of cadherin-23 and protocadherin-15 (Siemens *et al*, 2004; Sollner *et al*, 2004; Ahmed *et al*, 2006; Kazmierczak *et al*, 2007), may link ion channels at the tips of the stereocilia bundle where mechanotransduction takes place (Assad *et al*, 1991; Lumpkin and Hudspeth, 1995; Beurg *et al*, 2009). The tip link is necessary for mechanotransduction as shown by tip-link ablation experiments (Assad *et al*, 1991). Nevertheless, it is still unclear whether the tip link attaches directly to mechanosensitive ion channels or whether the tether molecule alters the force profile in the lipid bilayer around the channel (Kung, 2005). New evidence that rat hair cell mechanotransduction channels are predominantly located on the second and third row of stereocilia has ignited a debate as to whether tip links are directly connected to the transduction channels (Beurg *et al*, 2009; Spinelli and Gillespie, 2009).

The vast majority of mechanosensitive receptors in the body are sensory neurons of the dorsal root ganglia (DRG). Unlike hair cells, the mechanosensitive endings of sensory neurons are at a considerable distance from the cell body *in vivo*, in man this can be a distance of 1 m or more. Although the available evidence strongly suggests that mechanosensitive channels mediate the primary transduction event in mammalian sensory neurons, direct recording of transduction channel activity *in situ* has not been achieved (Hu *et al*, 2006). However, there are several examples of invertebrate mechanoreceptors in which the transduction current can be measured and these currents are necessary for mechanoreceptor function (Swerup *et al*, 1983; Hoger *et al*, 1997; O'Hagan *et al*, 2005). An alternative to recording transduction currents *in situ* is to measure the activity of mechanosensitive currents in acutely isolated sensory neurons (McCarter *et al*, 1999; Drew *et al*, 2002; Hu and Lewin, 2006; McCarter and Levine, 2006; Lechner *et al*, 2009). There is good evidence indicating that mechanosensitive currents

*Corresponding authors. GR Lewin or J Hu, Molecular Physiology of Somatic Sensation, Department of Neuroscience, Max-Delbrueck-Centrum, Robert-Rössle-Strasse 10, Berlin D-13125, Germany.
Tel.: +49 30 9406 2430; Fax: +49 30 9406 2793;
E-mail: glewin@mdc-berlin.de or Center for Integrative Neuroscience (CIN), Paul-Ehrlich-Strasse 15-17, Tubingen 72076, Germany.
Tel.: +49 7071 2989181; Fax: +49 7071 294697;
E-mail: jing.hu@cin.uni-tuebingen.de
[3]These authors contributed equally to this work
[4]Present address: Center for Integrative Neuroscience (CIN), Paul-Ehrlich-Strasse 15-17, Tübingen 72076, Germany

Received: 15 September 2009; accepted: 2 December 2009; published online: 14 January 2010

measured in acutely isolated sensory neurons are physiologically relevant for mechanoreceptor function *in vivo*. For example, deletion of the gene encoding stomatin-like protein-3 (STOML3 or SLP3) in mice leads to loss of mechanoreceptor function and abolishes mechanosensitive currents measured in isolated neurons (Wetzel *et al*, 2007). There are three distinct types of mechanosensitive currents in sensory neurons, which have been named according to their inactivation/adaptation kinetics, one is rapidly adapting (RA), one slow-adapting (SA) and one intermediately adapting (IA) (Hu and Lewin, 2006). The RA-mechanosensitive current has a very different ion permeability and pharmacology from that of the IA- and SA- mechanosensitive currents (Hu and Lewin, 2006; Drew *et al*, 2007). Indeed, all three types of mechanosensitive current appear at different time points during embryonic development and their appearance is regulated by different mechanisms (Lechner *et al*, 2009). The amplitude of the RA-mechanosensitive current in nociceptors has also been shown to be modulated by activation of G-protein-coupled receptors as well as through nerve growth factor signalling (Di Castro *et al*, 2006; Lechner and Lewin, 2009; Lechner *et al*, 2009).

In the present study we asked whether a tether model applies to mechanotransduction in mammalian DRG neurons that mediate our sense of touch. We subjected cultured sensory neurons to a range of different treatments that disrupt matrix–cell interactions and then measured the consequences for mechanosensitive currents. We found that treatment with specific proteases alone was capable of specifically abolishing the activity of the RA-mechanosensitive current. Using transmission electron microscopy (TEM) we showed that such treatments also specifically ablate a large protein tether (~100 nm) that links sensory neuron membranes to a laminin matrix. The loss and reappearance of mechanosensitive currents was always linked to the presence of this tether. Experiments performed using intact skin-nerve preparation demonstrated that proteolytic cleavage specifically ablates the mechanosensitivity of touch receptors and thus reproduces the effects observed *in vitro*. Our study shows that extracellular links are necessary for the mechanosensitivity of somatic sensory afferents.

Results

Only the terminal endings of sensory neurons in the skin are mechanosensitive *in vivo*, and we thus sought to establish an *in vitro* model of the cellular milieu found at the receptor ending. To this end, adult mouse sensory neurons were cultured on a monolayer of mouse 3T3 fibroblasts. Sensory neurons grow neurites on fibroblasts and mechanical stimulation of these neurites (750 nm amplitude displacement) evoked fast mechanosensitive currents, as measured using whole-cell recording from the nearby cell body (Figure 1A and B). Using such stimuli it was observed that >98% of isolated sensory neurons ($n=45$) possessed one of three mechanically activated currents, RA (inactivation in <5 ms), IA (inactivation in <50 ms) and SA (no adaptation during a 230 ms stimulus) (for examples see Figure 2A). Indeed the amplitude and kinetic parameters of neuritic mechanosensitive currents were identical to those observed on a standard laminin substrate obtained from matrix derived from Engelbreth–Holm–Swarm (EHS) cells (Invitrogen) (Figure 1A and B) (Hu and Lewin, 2006). We hypothesized that if mechanosensitive ion channels are gated by a tether linking them to the fibroblasts or matrix surrounding the fibroblast, then mechanical displacement of the fibroblast adjacent to the neurite may evoke fast mechanosensitive currents in sensory neurons. We found that in almost all cases (16/17 neurons) short-latency, fast-activating mechanosensitive currents were indeed evoked in sensory neurons when adjacent fibroblasts were mechanically stimulated (Figure 1A and B, and Supplementary Video S1). Compared with direct stimulation of neurites, the latency and activation time constant of the mechanosensitive current was virtually identical after mechanical stimulation of the adjacent fibroblast (Figure 1B). Most of the neurons recorded with a fast-evoked mechanosensitive current in response to mechanical stimulation

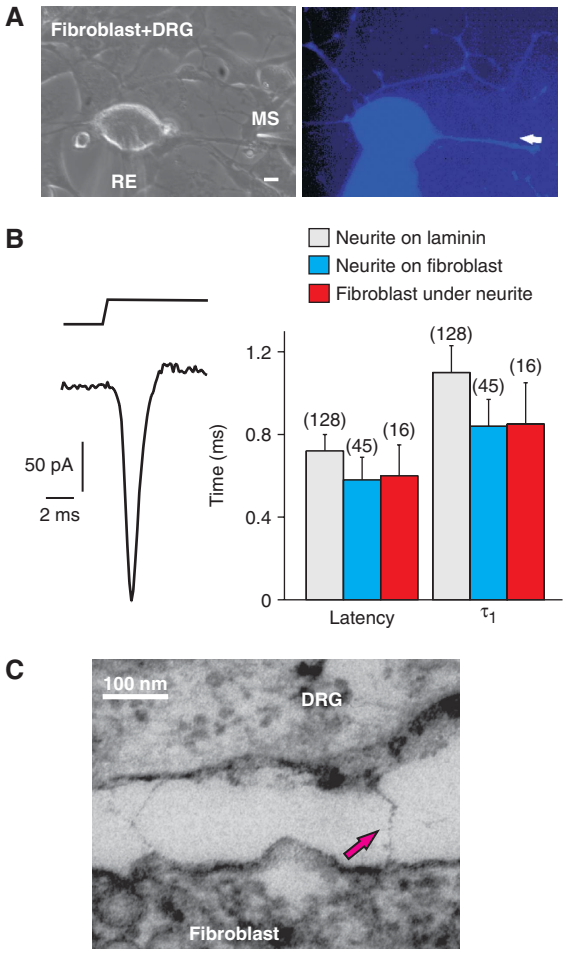

Figure 1 Fibroblast/sensory neuron co-cultures suggest a tether gating mechanism. (**A**) Bright-field (left) and fluorescence micrograph (right) of a recorded neuron on fibroblasts, filled with Lucifer Yellow from the recording pipette (RE). Mechanical stimuli (MS, amplitude 750 nm) were applied either to the neurite directly or to the adjacent fibroblast (indicated by white arrow). (**B**) Example of an RA-mechanosensitive current in a sensory neuron evoked by a 750-nm displacement of a fibroblast adjacent to the neurite. The bar graph shows the mean latency and mean activation time constant τ_1 (obtained from mono-exponential fits of the current trace) for the mechanosensitive current evoked from the neurite on laminin (grey), neurite on fibroblast (blue) and from the fibroblast underneath the neurite (red). (**C**) Electron micrograph of electron-dense filaments observed between neurites and fibroblasts in a sensory neurons/fibroblast co-culture. Error bars represent the s.e.m.

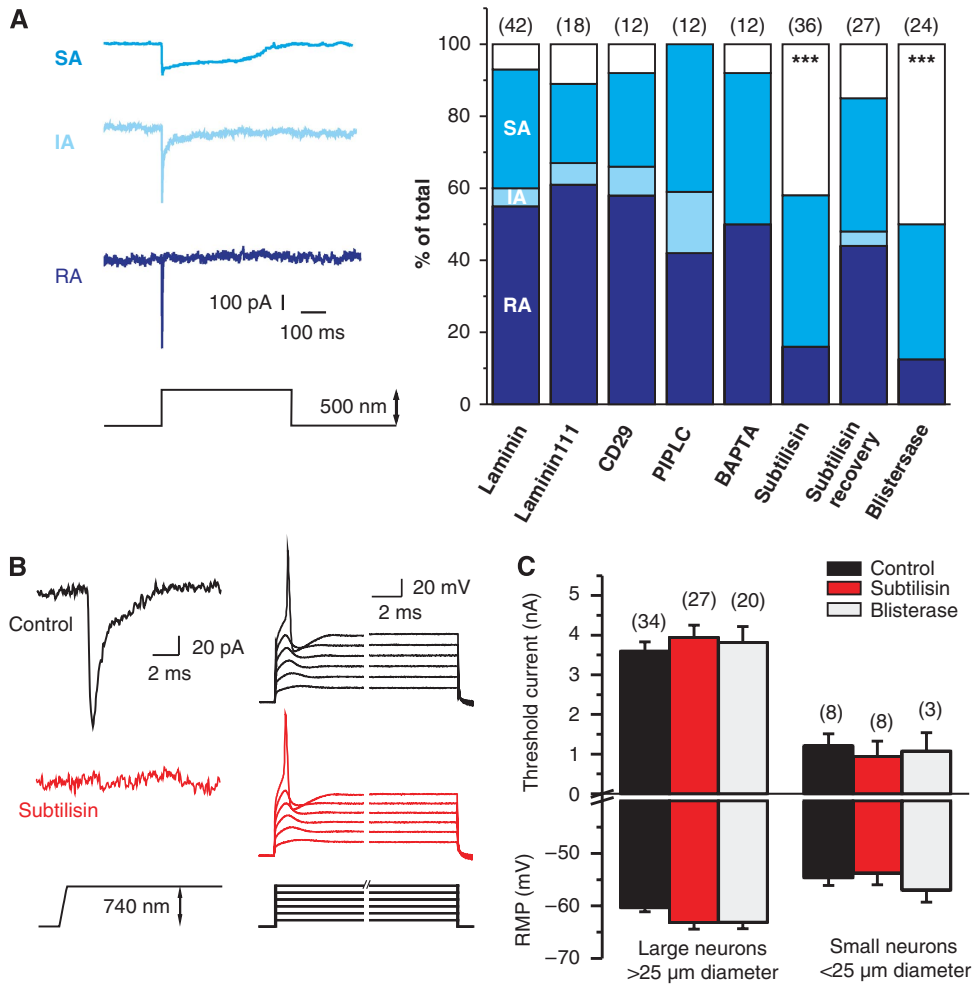

Figure 2 Subtilisin and blisterase selectively abolish RA-mechanosensitive currents. (**A**) Examples of RA-, IA- and SA-mechanosensitive currents evoked by stimulating sensory neuron neurites. Stacked histograms of the proportion of the three types of mechanosensitive current observed in controls (laminin and laminin-111) as compared with those in cultures treated with agents that disrupt extracellular matrix–cell interactions. The number of recorded neurons is indicated at the top of each stacked histogram. The empty bars indicate neurons in which no mechanosensitive current could be measured. (**B**) Local perfusion of single neuron with subtilisin leads to complete loss of the RA-mechanosensitive current (left); the current injection is, however, still effective at initiating APs. (**C**) The resting membrane potential (RMP), and the threshold current for AP initiation, was measured 0–3 h after subtilisin (red bars) or blisterase treatment (grey bars); the data were analysed separately for large (>25 µm diameter) and small neurons (<25 µm diameter); no differences were noted as compared with controls (black bars). Error bars represent ± s.e.m.

of adjacent fibroblasts, had an RA-mechanosensitive current (10/16). However, we also recorded fast SA- and IA-mechanosensitive currents in response to fibroblast stimulation (4 SA, 2 IA). The fact that the latency and activation of the mechanosensitive current evoked by stimulation of the neurite or adjacent fibroblast was not different, suggests that a physical link might transfer force from the stimulated fibroblast to mechanosensitive ion channels in the sensory neuron.

We next prepared sensory neuron/fibroblast co-cultures for TEM using fixation and staining procedures optimized to visualize extracellular proteins (see section Materials and methods). At the ultrastructure level we were able to distinguish fibroblast cells from neuronal profiles by the presence of neurofilament and the high density of mitochondria in sensory cells. Careful examination of many TEM sections revealed occasional long, tether-like links between fibroblasts and sensory neurites (Figure 1C). Such tethers are candidate entities for transferring force from matrix produced by fibroblasts and mechanosensitive channels. Electron microscopy was, however, challenging in this mixed culture system and clearly identifiable neurite/fibroblast interfaces were rare. Our data showed that the physiological properties of the mechanosensitive currents are indistinguishable when measured from neurons in neuron/fibroblast co-cultures or on laminin substrates (Figure 1B). We thus reasoned that if protein tethers are relevant for the function of mechanosensitive currents, they should also be present in sensory neurons cultured on laminin substrates (see below). We measured mechanosensitive currents in sensory neurons cultured on laminin (EHS-derived) as well as on laminin-111, a highly purified, trimeric laminin-$\alpha_1\beta_1\gamma_1$–nidogen complex (Paulsson *et al*, 1987). We found that the incidence of mechanosensitive currents, their kinetic properties and amplitudes were not different between neurons plated on laminin or laminin-111 (Figure 2A). We also measured the mechanosensitive current in neurons plated only on a poly-L-lysine substrate (PLL); such neurons attach poorly and only some neurons actually extend neurites (data not shown). We found that 43% (8/17 neurons tested) lacked mechanosensitive currents when plated on the PLL substrate, a proportion

substantially higher than that found on laminin, which was 7% (3/42 neurons tested), and this was significant, with $P<0.05$ on χ^2-test. We also noted that in cases where a mechanosensitive current was measured, there was always a nearby fibroblast that may have secreted a laminin-containing substrate.

We next conducted a series of experiments to examine the effects of manipulating extracellular matrix integrity or matrix–cell interaction on the mechanosensitive current measured in neurons plated on laminin. Hair cell tip-link proteins are rapidly disrupted by Ca^{2+} chelation, consistent with the calcium dependence of cadherin interactions (Assad *et al*, 1991; Zhao *et al*, 1996; Siemens *et al*, 2004; Sollner *et al*, 2004; Kazmierczak *et al*, 2007). However, depleting extracellular Ca^{2+} ions with the calcium chelator 1,2-bis(*o*-aminophenoxy)ethane-*N*,*N*,*N*,*N*-tetraacetic acid (BAPTA) for 30 min had no effect on the incidence of the three types mechanosensitive currents. Indeed we, like others, noted that the amplitude of mechanosensitive current increased after exposing neurons to calcium-free solutions (Supplementary Table S1), which is consistent with partial calcium block of the mechanosensitive channel (Drew *et al*, 2002; Lechner *et al*, 2009). It has been suggested that integrin receptors might play a role in the transduction of mechanical stimuli in sensory neurons (Khalsa *et al*, 2004); we therefore blocked integrin signalling with the CD29 antibody (Mendrick and Kelly, 1993; Tomaselli *et al*, 1993). However, such treatments had no effect on the incidence or kinetic properties of mechanosensitive currents. A large number of membrane proteins are known to be glycosyl phosphatidylinositol (GPI)-anchored (Kinoshita *et al*, 2008), and some of them, like the channel-activating protease, (CAP1) can regulate mechanotransduction-related channels (Vallet *et al*, 1997). We thus used the enzyme phosphatidylinositol-specific phospholipase-C (PIPLC) to cleave GPI anchors from the membrane. A large number of membrane proteins are thought to be GPI-anchored (Kinoshita *et al*, 2008), but this treatment again did not affect the kinetic properties, integrity and proportion of cells with a mechanosensitive current in sensory neurons (Figure 2A and Supplementary Table S1).

To address the possibility that an extracellular protein may be required for mechanosensitive current function, neurons in culture were subjected to limited proteolysis using soluble proteases. We first locally treated sensory neurons with the non-specific endopeptidase subtilisin during the recordings. Within 5–30 min after the start of local application of subtilisin at room temperature (50 μg ml^{-1}), the RA-mechanosensitive current completely disappeared ($n=7/8$ tested with an RA-mechanosensitive current). In contrast, under identical experimental conditions, three neurons with an SA-mechanosensitive current were unaffected by local subtilisin treatment (Figure 2B). After loss of the RA-mechanosensitive current, the threshold current for AP initiation in current clamp mode was unchanged as compared with pretreatment values (Figure 2B and C).

We also used the subtilisin-related, site-specific protease blisterase from *Onchocerca volvulus*, which cleaves a tetrabasic sequence with the motif RX(K/R)R (Poole *et al*, 2003) We conducted experiments using populations of cells pretreated with subtilisin (50 μg ml^{-1}, 120 s, 37°C) or blisterase (10–75 U ml^{-1}, 5–200 min, 37°C) and found that between 0 and 3 h after treatment, the proportion of cells found with an RA-mechanosensitive current was reduced from 55% (23/42 cells) in the control to just 16% (6/36 cells) in subtilisin-treated cultures, and 12.5% (3/24) in blisterase-treated cells (χ^2-test $P<0.001$) (Figure 2A). After subtilisin or blisterase treatment, 70–80% of the cells with a large cell body and a narrow AP, characteristic of mechanoreceptors, lacked a mechanosensitive current (subtilisin 8/10 tested; blisterase 7/10 tested). In control cultures, all mechanoreceptors possessed an RA-mechanosensitive current (19/19 cells with narrow APs tested) (Hu and Lewin, 2006) (see Supplementary Figure S1). Many of the cells lacking mechanosensitive currents after subtilisin or blisterase treatment (subtilisin 7/15 tested; blisterase 5/12 tested) were putative nociceptors with humped APs (Koerber *et al*, 1988; Lewin and Moshourab, 2004). The electrical excitability of the non-mechanosensitive cells was normal, as measured by the resting membrane potential, the amplitude of the AP and the threshold current needed to evoke an AP in a current clamp (Figure 2B and C). The current–voltage (I–V) relation for inward and outward currents was also not substantially altered by prior blisterase or subtilisin treatment (Figure 3A and B). However, neurons pretreated with subtilisin exhibited a slight, but significant, shift in the mean activation threshold for voltage-gated inward currents to more negative potentials (Figure 3B). These data suggest that voltage-gated ion channels are not substantially altered by subtilisin cleavage at the concentrations and incubation times used here. Blisterase had no discernable effect on the inward or outward voltage-gated currents in the cells measured (Figure 3B). In addition, transient and sustained proton-gated currents, which may be mediated, in part, by acid-sensitive ion channels (ASICs), which have very large extracellular domains (Kellenberger and Schild, 2002; Jasti *et al*, 2007), were not changed in amplitude after subtilisin or blisterase treatment (Figure 3C and D). The number of neurons with an SA-mechanosensitive current remained unchanged after subtilisin and blisterase treatment (Figure 2A). The SA-mechanosensitive current is found exclusively in nociceptors and is developmentally, pharmacologically and biophysically distinct from the RA-mechanosensitive current (Hu and Lewin, 2006; Drew *et al*, 2007; Lechner *et al*, 2009). It should be noted that we also found no neurons with an IA-mechanosensitive current after pretreatment with subtilisin or blisterase, although one neuron with an IA-mechanosensitive current was recorded in the subtilisin recovery experiment (see below) (Figure 2A). However, the very low incidence of the IA-mechanosensitive current in the control cultures means that it is not possible to reliably evaluate whether the IA current also relies on the presence of a protease-sensitive extracellular protein.

The blisterase enzyme is derived from the pathogenic nematode *O. volvulus*, but has been shown to have essentially the same substrate specificity as the human furin enzyme (Nakayama, 1997; Poole *et al*, 2003). We therefore conducted a series of experiments where we treated sensory neuron cultures with a soluble truncated human furin enzyme (Bravo *et al*, 1994). We found that at similar concentrations to blisterase (100 U ml^{-1}, 25–45 min, 37°C), pre-incubation of cultures with furin led to significant and substantial loss of RA-mechanosensitive current in mechanoreceptors. Thus, 8/13 neurons with APs characteristic of mechanoreceptors completely lacked the mechanosensitive current after prior furin treatment, and this was significantly different from that

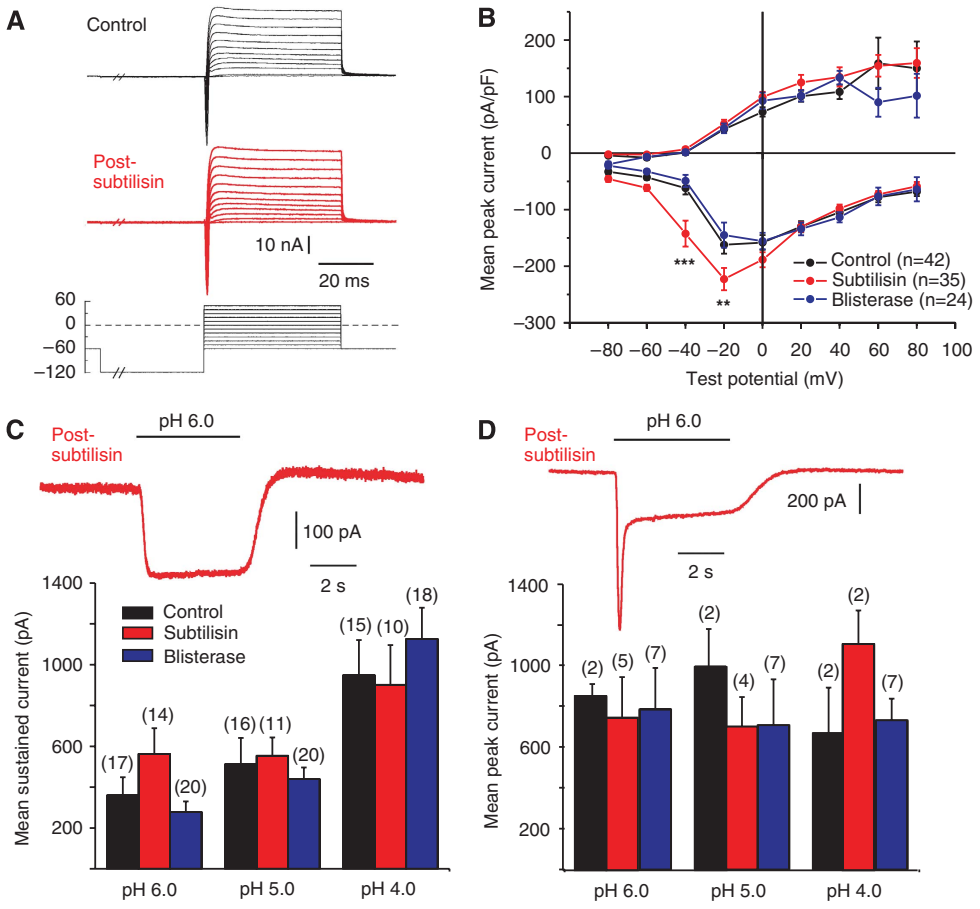

Figure 3 Protease treatment does not affect other ion channels. (**A**) Example traces of whole-cell currents evoked by a series of step depolarization steps from a −120-mV pre-pulse potential in 10-mV steps, to +50 mV. The black traces are from the neurons before subtilisin treatment and the red traces were obtained post-subtilisin; no major change was seen in the kinetics or amplitudes of inward and outward currents. (**B**) Mean whole-cell inward and outward currents measured at different test potentials for all control cells (black) and cells treated acutely with subtilisin (red) or blisterase (blue). At each test potential, the peak inward current peak outward current at steady state was measured. Neurons treated with subtilisin showed small, but significant, leftward shift in the voltage for peak activation of the inward current (asterisks indicate data points significantly different from the control; two-way ANOVA, Bonferroni *post hoc* test $P>0.01$). No change was observed in blisterase-treated cells as compared with that in the controls. (**C**, **D**) Proton-gated currents are not altered after subtilisin and blisterase treatment. The peak sustained (example trace in panel **C**) and transient (example trace in panel **D**) were not altered after subtilisin treatment. The amplitudes of proton-gated currents measured with stimuli of pH 6.0, 5.0 and 4.0 were not significantly different between control (black), subtilisin-treated (red) and blisterase-treated (blue) cells. The numbers of cells measured in each group is indicated in parentheses above each column.

in the control cultures (0/19 mechanoreceptors lack the mechanosensitive current, χ^2-test $P<0.001$). We also used 10 times lower concentrations of the furin enzyme (10 U ml^{-1}, up to 900 min, 37°C), but found no significant effect on the presence of mechanosensitive currents (data not shown). It appears that the two site-specific proteases, blisterase and furin, have very similar effects. We used the blisterase enzyme in further experiments as this enzyme appeared to be slightly more efficient than furin.

Following ablation of the hair cell tip link, mechanotransduction is lost, but transduction currents return 24 h later, correlated with the appearance of new tip-link proteins to the bundle (Zhao *et al*, 1996). We measured mechanosensitive currents in populations of cells 17–30 h after subtilisin removal. At these time points the incidence of the RA-mechanosensitive current had returned to control values and the latency and kinetics of these currents were identical to those in the controls (Supplementary Table S2). Thus, since sensory neurons are the major cell type in the culture, it appears that the cleaved extracellular peptide can be re-inserted into the membrane after cleavage to reinstate mechanosensitive current function. Recordings made at intermediate time points after subtilisin treatment did not show full recovery of the mechanosensitive current (data not shown).

We next asked whether anatomically identifiable protein tethers, that are subtilisin/blisterase-sensitive, could be responsible for RA-mechanosensitive current gating. We performed a quantitative TEM analysis comparing electron-dense attachments between the sensory neurite membrane and the laminin substrate under five conditions: control, subtilisin-treated acute (3 min) or subtilisin-treated 30-h recovery, blisterase-treated acute (25 min) and PIPLC treated (120 min). We could visualize an electron-dense laminin matrix 17 ± 1 nm in depth on the surface of the culture dishes, with a variety of tight and loose electron-dense connections between the neurite membrane and the matrix (Figure 4B). The longest connecting objects were similar in length (~100 nm) and shape to those observed in TEM of sensory neuron/fibroblast co-cultures (Figures 1C and 4B). The longest protein tethers were very rarely observed in subtilisin- or

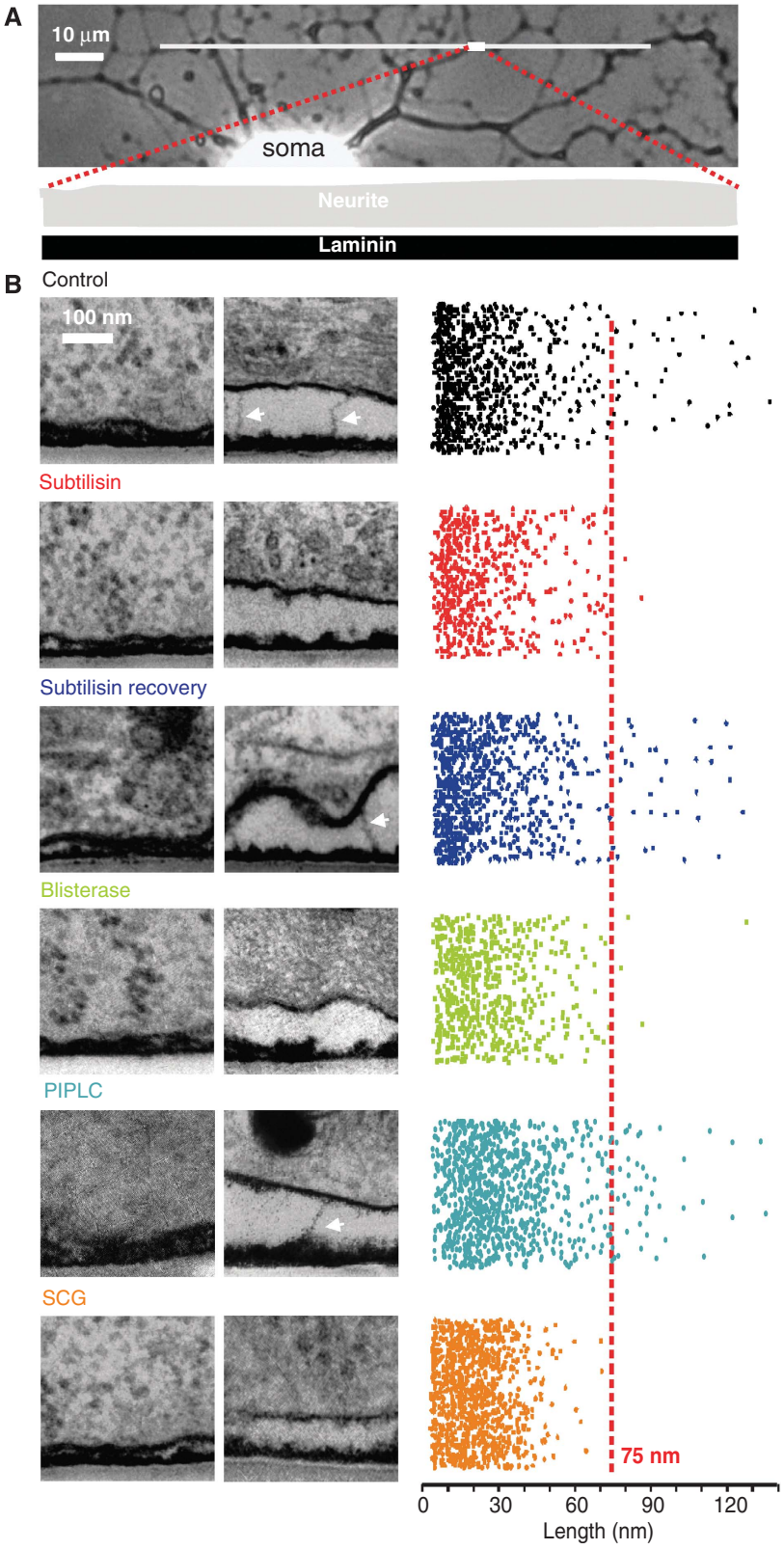

Figure 4 TEM reveals a protein filament necessary for mechanotransduction. (**A**) Light photomicrograph of a cultured sensory neuron with a neuritic tree. The TEM photomicrographs were generated from ultrathin sections from blocks of tissue, with dimensions in the range illustrated by the white rectangle at the end of red dotted lines. (**B**) Sample electron micrographs of the neurite–matrix interface under a series of conditions, including, in each case, a quantification of the length of each measured attachment plotted in random two-dimensional space to illustrate the range of attachment lengths observed (right). Objects larger and smaller than 75 nm are demarcated by the red line. For each experimental condition, two sample photomicrographs are shown: one field illustrating tight attachment of the plasma membrane to the substrate and one a looser attachment area, with or without long protein tethers. For each experimental condition, a colour code is applied as follows: from the top, control (black), subtilisin acute (red), subtilisin recovery (purple), blisterase treatment acute (green), PIPLC treatment acute (cyan) and SCG neurons on laminin (orange).

blisterase-treated cultures, but the incidence was essentially the same in the control and subtilisin-treated 30-h recovery group (Figure 4B). We quantified these data by randomly photographing microscopic fields in between 58 and 99 ultrathin sections (thickness 50 nm) from two to four cultures in each group and measured the number and length of the electron-dense objects that linked the neurite membrane to the laminin substrate (see Supplementary Table S3). The measured area of membrane contact was between 4.66 and 9.42 μm^2 in each group; the length of each object was then randomly plotted in two-dimensional space (Figure 4B). It is obvious from this representation of the raw data, that links with length between 5 and 75 nm were largely unaffected by subtilisin/blisterase treatment. However, electron-dense objects >75 nm in length, presumably corresponding to protein filaments, were selectively abolished after subtilisin/blisterase treatment (Figure 4B), but reappeared in cultures allowed to recover for 30 h after subtilisin treatment (Figure 4B). The final PIPLC-treated group served as control for enzymatic digestion of the sensory neuron culture *per se*. Electron-microscopic analysis of such cultures revealed no change in the incidence of filaments >75 nm (Figure 4B); nevertheless there was a significant shift in the mean size of electron-dense objects <75 nm in length (Supplementary Table S3), which probably reflects the shedding of a diverse group of GPI-anchored membrane proteins. It is conceivable that mechanosensitive currents are lost after protease treatment because of neurite detachment from the culture dish. If this were so then the long tether may be lost not because of proteolysis, but rather because of membrane detachment. To control for this possibility, all the sections were analysed to measure the average interface distance between the neurite membrane and the laminin substrate. As can be seen in the example electronmicrographs in Figure 4B, the physical distance can vary considerably along the contact zones. We found no significant difference between the mean neurite/laminin interface distance of 77 ± 8 nm in the control cultures as compared with 99 ± 8 nm in subtilisin-treated cultures and 80 ± 6 nm in blisterase-treated cultures ($P > 0.05$, Student's *t*-test). We and others have previously shown that RA-mechanosensitive currents can readily be evoked by stimulation of the cell soma (McCarter *et al*, 1999; Drew *et al*, 2002, 2004; Hu and Lewin, 2006; McCarter and Levine, 2006; Lechner and Lewin, 2009; Lechner *et al*, 2009), and this raises the question whether the tether protein identified here is present at the soma–laminin interface. However, we were in fact able to observe tether-like filaments at soma–laminin interfaces (see example in Supplementary Figure S2); thus, stimulation of the soma may also gate mechanosensitive currents via an extracellular protein tether.

The subtilisin/blisterase-sensitive protein filament identified in our TEM experiments may be necessary for the gating of the RA-mechanosensitive current. To further test whether the long protein tether is specifically associated with the RA-mechanosensitive current, we recorded from superior cervical ganglion neurons (SCG) cultured on laminin. Sympathetic neurons are autonomic efferent neurons that have been reported not to possess mechanosensitive currents (Drew *et al*, 2002). We could confirm that no RA-mechanosensitive currents are observed in any of the recorded SCG neurons (Figure 5A). We did, however, observe small-amplitude, SA-mechanosensitive currents in sympathetic neurons at a very low frequency (13%, 2/15 neurons) (Figure 5A and B). A detailed TEM study showed that no extracellular protein filaments are found that are greater than 75 nm in length, in SCG neuronal cultures (Figure 4B). Thus, among peripheral neurons it is only sensory neurons with a mechanosensory function that appear to synthesize a long tether-like protein when cultured on a laminin substrate.

In summary, our data suggest a model where a subtilisin/blisterase-sensitive protein filament links mechanosensitive ion channels in the membranes of sensory neurons to a laminin-containing matrix. Measurement of electron-dense objects longer than 75 nm in sensory neuron cultures showed that these long protein filaments average 100 ± 3 nm in length and occur with an average density of 4.9 ± 1.3 filaments per μm^2 of membrane (Supplementary Table S3). The tether-like protein is synthesized by sensory neurons as demonstrated by its recovery after 17–30 h in cultures briefly treated with the subtilisin protease. TEM analysis shows that one end of the filament attaches to the laminin-containing matrix. The fact that the tether-like protein is present when the RA-mechanosensitive currents are functioning and is absent or much reduced in situations where the RA-mechanosensitive

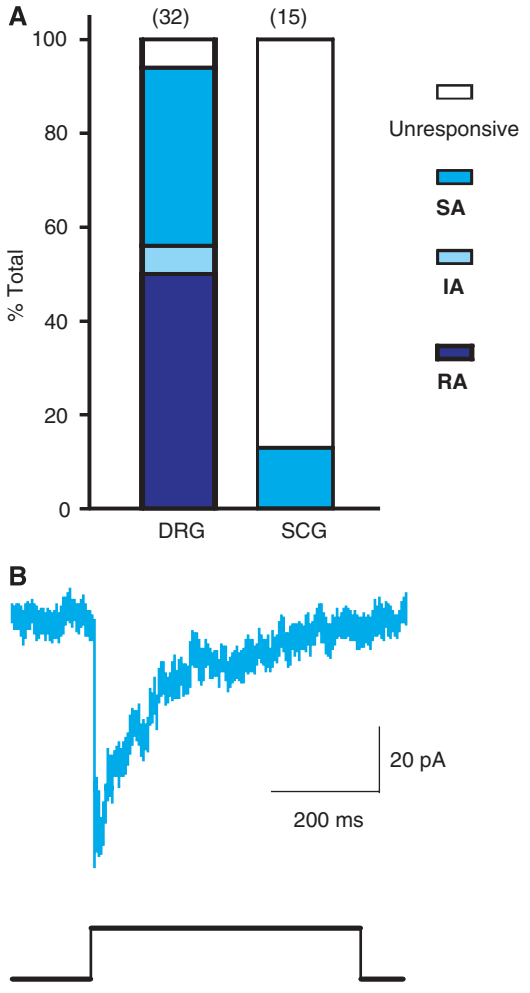

Figure 5 Superior sympathetic neurons lack an RA-mechanosensitive current (**A**). A stacked histogram of the proportion of three types of mechanically activated currents designated RA (dark blue), SA (medium blue) or IA (light blue) observed in DRG neurons and SCG neurons. (**B**) Example of an SA-mechanosensitive current recorded in an SCG neuron.

current is also reduced, suggests that this protein is likely necessary for the gating of the RA-mechanosensitive current. Further strong evidence for a mechanosensory role for this protein is the fact that peripheral non-mechanosensory neurons, lacking an RA-mechanosensitive current, do not synthesize tether-like proteins >75 nm in culture (Figures 4 and 5).

The question arises whether subtilisin-sensitive protein filaments may be required for mechanoreceptor function *in situ*. We applied the subtilisin enzyme (50 μg μl^{-1}) to the receptive fields of single identified mechanoreceptors and nociceptors recorded using the *in vitro* skin-nerve preparation (Martinez-Salgado *et al*, 2007; Milenkovic *et al*, 2008). When using a standard supra-threshold mechanical stimulus (ramp and hold displacement between 48 and 96 μm, for 2 s every 60 s), the mechanoreceptor response in most neurons remained very stable for periods greater than 20 min up to 90 min (data not shown). However, between 3 and 8 min after application of subtilisin enzyme, 50% of all the low-threshold mechanoreceptors displayed no mechanosensitivity (Figure 6A). The median survival time for the loss of mechanosensitvity was shortest for RA and SA mechanoreceptors (SAMs and RAMs) at 3–4 min and longest for D-hair mechanoreceptors at 8 min (Figure 6B). By the end of the observation period, virtually all mechanoreceptors were mechanically insensitive. For each treated afferent included in this analysis, electrical stimulation with a metal electrode placed in the receptive field at the end of the experiment evoked the same spike as was observed before commencement of treatment. Thus mechanosensitivity, but not electrical excitability, was abolished by subtilisin treatment (Figure 6A). In contrast, when mechanosensitive nociceptors with Aδ-axons were subjected to the same protocol, no effect on mechanosensitivity was observed (Figure 6B). In addition to being observed in mechanoreceptors, the RA-mechanosensitive current is also observed in a proportion of small sensory neurons *in vitro* that probably give rise to C-fibre nociceptors (Hu and Lewin, 2006; Lechner and Lewin, 2009). Consistent with this finding, we found that the mechanosensitivity of some, but not all, C-fibre nociceptors was attenuated by subtilisin treatment; however, this effect did not reach statistical significance (Figure 6B). The data from all the skin-nerve preparation experiments were also analysed in terms of the mean spike response per stimulus before and after application of subtilisin and the results were found to be similar (Supplementary Figure S3).

SA-mechanosensitive currents are found exclusively in nociceptors (Hu and Lewin, 2006) and the incidence of these currents and their kinetic properties were largely unaffected by protease treatment (Figure 2). However, SA-mechanosensitive currents were not completely insensitive to protease treatment as the mean latency for current activation more than doubled in neurons pretreated with subtilisin, blisterase and furin (even at the lower dose of 10 U ml^{-1}) (Figure 7A and B). The latency measured for the SA-mechanosensitive current had recovered to control values after a 17- to 30-h recovery period. Thus, subtilisin/blisterase-sensitive polypeptides are necessary for the normal kinetics of the SA current, but are not required for current activation. After treatment of the receptive field in the skin with subtilisin most C-fibres do not lose mechanosensitivity (Figure 6). However, we also monitored the mechanical latency of the responses during the course of the experiment. Mechanical latency is the time from the onset of the ramp stimulus until the first spike corrected for conduction delay and is a good measure of the mechanical threshold (Milenkovic *et al*, 2008). In control experiments the mechanical latency of C-fibre responses is always stable with repeated supra-threshold stimuli (Figure 7C). However, in subtilisin-treated C-fibres the mean mechanical latency increased steadily and significantly during the course of the treatment (Figure 7C). The increased mechanical latency in single C-fibres is reminiscent of the increased latency of the mechanosensitive current that we observed after subtilisin/blisterase/furin treatment *in vitro* (Figure 7A and B). The change in mechanical latency observed in C-fibres after subtilisin was not observed in other afferent fibres including Aδ-mechanonociceptors (AM) (Supplementary Figure S4).

Discussion

In this paper we provide direct evidence that mechanosensitive channels, which underlie vertebrate touch sensation, require an extracellular tether protein to function. Genetic screens for touch-insensitive worms have revealed alleles of the *mec* genes that encode putative extracellular proteins (Gu *et al*, 1996; Emtage *et al*, 2004). Also mutant flies lacking mechanoreceptor potentials harbour mutations in the *NompA* gene that encodes a large extracellular protein that may be well-positioned to interact with transduction channels in bristle sensory neurons (Chung *et al*, 2001). However, the extracellular proteins identified in such genetic screens have not been shown to interact directly with transduction channels (Cueva *et al*, 2007) and may instead play a structural or organizing role (Chung *et al*, 2001; Emtage *et al*, 2004). Indeed if such proteins act as gating tethers then acute ablation of the protein should abolish mechanotransduction as demonstrated in vertebrate hair cells (Assad *et al*, 1991; Zhao *et al*, 1996; Goodyear and Richardson, 2003; Siemens *et al*, 2004; Kazmierczak *et al*, 2007), but such experiments have not yet been conducted using model organisms such as worms and fruit flies.

The situation for mechanoreceptors that mediate touch sensation in vertebrates was unknown. However, here we demonstrate that mechanosensitive currents that are necessary for mechanoreceptor function (see Supplementary Figure S1) only work in the presence of an extracellular subtilisin/blisterase/furin-sensitive protein tether. Thus, under three experimental conditions (acute subtilisin, acute blisterase and in cultured sympathetic ganglion neurons) no or few neurons are recorded with an RA-mechanosensitive current and few or no tethers >75 nm are observed. In contrast, there were three other situations where tethers were observed and so were RA-mechanosensitive currents (control, subtilisin recovery and PIPLC treatment). We were also able to demonstrate that loss of the RA-mechanosensitive current can happen within a few minutes of exposure to the endopeptidase subtilisin (Figure 2A). This striking finding strongly suggests that a subtilisin-sensitive polypeptide is directly involved in maintaining the function of the RA-mechanosensitive current. It might be argued that the functionally important peptides that are cleaved by subtilisin and blisterase are not identical to the ~100-nm-long tether that we have identified in our TEM studies. However, the fact

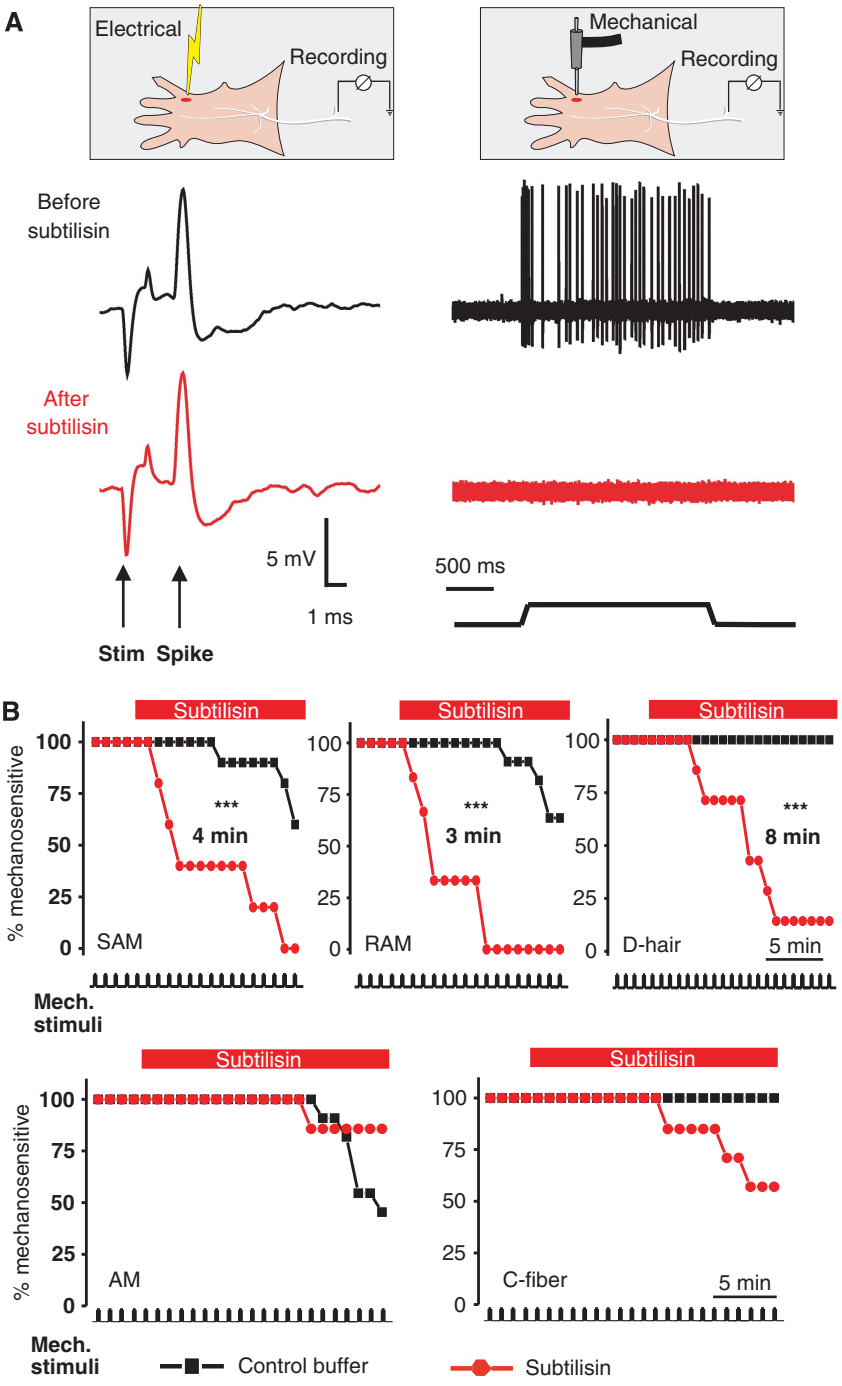

Figure 6 Mechanoreceptors, but not nociceptors, require a subtilisin-sensitive protein. (**A**) A schematic representation of the recording setup using the *in vitro* skin-nerve preparation and an example of a recording from a mechanoreceptor (SAM) before (black trace) and after application of subtilisin locally to the receptive field (red trace). Note that the electrically evoked spike is unaffected by the treatment, but the fibre's mechanosensitivity was completely abolished. (**B**) Kaplan–Meyer plots of the percentage of sensory fibres with a mechanosensitivity before and after local application of subtilisin. The top row contains data from three types of mechanoreceptor (RAM, SAM and D-hair are shown; note that subtilisin abolishes mechanosensitivity in all three receptors, with a median survival time as indicated). The bottom row shows the same experiment for A-fibre nociceptors (AMs) and for nociceptive C-fibres; no significant effect of subtilisin was observed. *** indicates statistical significance ($P<0.005$ log-rank test).

that non-mechanosensory sympathetic neurons also do not synthesize a 100-nm-long tether protein lends further support to the idea that this entity is functionally relevant for RA-mechanosensitive currents. A further possibility is that the protease treatments we have used here cleave the mechanosensitive channel directly and we cannot exclude such a possibility at the present time. However, we have demonstrated that the function of a variety of voltage-gated and ligand-gated ionic currents was largely unaffected by the protease treatments used (Figure 3), and this includes putative ASIC-like currents that are mediated by ion channels with a very large extracellular polypeptide.

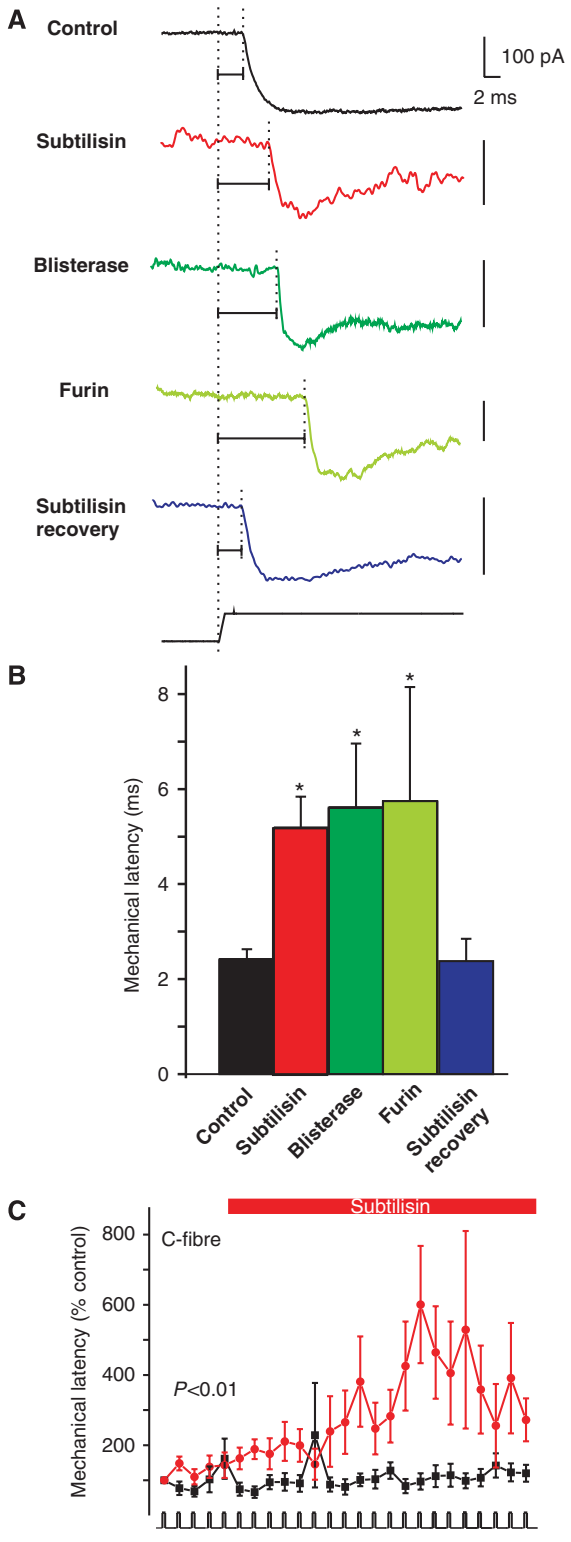

Figure 7 Protease modulation of transduction speed. (**A**) The latency of the SA-mechanosensitive current was measured in controls and protease-treated cells. Note that all protease treatments led to clear increase in the mechanical latency of the current (horizontal lines) as compared with that in the control (black trace), and this recovered to control values after recovery (blue trace bottom). Note that all vertical scale bars denote 100 pA. (**B**) Quantification of data shown in panel **A**; all three protease treatments lead to increased latency of the SA-mechanosensitive current. (**C**) The mechanical latency of C-fibre nociceptors treated at the receptive field with subtilisin is significantly increased following the application in the skin-nerve preparation. Statistical significance was calculated by repeated-measures ANOVA.

We show that mechanoreceptor function *in vivo* is also dependent on a protease-sensitive extracellular polypeptide. The effects of subtilisin treatment on mechanoreceptor function were remarkably specific in that the mechanosensitivity of single mechanoreceptors was rapidly (<3 min) abolished, but electrical excitability was completely preserved (Figure 6A). So far this is the first example of any treatment, pharmacological or otherwise, that can specifically ablate the mechanosensitivity of cutaneous afferents *in vivo*. The effects of subtilisin treatment in the intact skin also mirrored those observed *in vitro* in that nociceptor mechanosensitivity was largely preserved (Figure 2). Interestingly, the mechanical latency of C-fibre nociceptors increased substantially during subtilisin treatment and this phenomenon is reminiscent of the increased latency for the SA-mechanosensitive current observed following subtilisin treatment *in vitro* (Figure 7). We have previously shown that the mechanical latency of C-fibre nociceptors is surprisingly long as the fastest latency achieved *in vivo* is ~100 ms, which is an order of magnitude slower than the time to evoke an SA-mechanosensitive current *in vitro* (Milenkovic *et al*, 2008). The discrepancy between the long mechanical latencies observed for C-fibres *in vivo* and the relatively fast mechanosensitive currents measured in nociceptors remains unexplained. However, it should be noted that the mechanical latency *in vivo* directly reflects changes in mechanical threshold as well as the speed of transduction. Thus the elevation in mechanical latency observed after subtilisin treatment may accompany a higher threshold for gating of the SA-mechanosensitive current. The mode of mechanical stimulation that we have used here to evoke mechanosensitive currents is usually supra-threshold and so changes in threshold would not necessarily be detected using our experimental design. Together our data suggest that a protease-sensitive extracellular element is involved in regulating the mechanosensitivity of many nociceptors, but is not essential for mechanotransduction in these afferent fibres. However, there remains the possibility that like in the hair cell there are extracellular proteins that are not readily cleaved even by the non-specific protease subtilisin (Osborne and Comis, 1990; Goodyear and Richardson, 1999).

Stretch-activated channels have been characterized in many cell types (Guharay and Sachs, 1984; Lane *et al*, 1991) and recent evidence suggests that a stretch-activated cation channel (SAC) is regulated by members of the TRP-channel family (Sharif-Naeini *et al*, 2009). However, the role of SACs in mechanoreceptors has been controversial (Morris and Horn, 1991; Cho *et al*, 2002) and our data show that it is unlikely that membrane stretch, by itself, is sufficient to gate mechanosensitive channels required for touch perception. However, it is intriguing that the SA current, found exclusively in nociceptors (Hu and Lewin, 2006; Lechner *et al*, 2009), appears largely insensitive to extracellular proteolysis both *in vitro* and *in vivo* (Figures 2 and 6). Interestingly, at least three types of SACs with different thresholds and single-channel conductance have been recorded by Oh and workers in the membranes of nociceptive sensory neurons (Cho *et al*, 2002, 2006). It is not clear at the moment whether these SACs underlie the SA-mechanosensitive current that we and others have recorded to direct mechanical stimulation (Drew *et al*, 2002, 2004, 2007; Hu and Lewin, 2006). Nevertheless, we provide evidence here that the kinetics of the SA-mechanosensitive current is dependent on protease sensitive link to

the extracellular matrix (Figure 7). It may be that protease-sensitive extracellular links to SACs or related channels have a primary role in increasing the speed of mechano-electric transduction, and this interpretation would be supported by our data (Figure 7).

The protein filament that we have identified is synthesized by sensory neurons and appears to have a constant length of ~100 nm and can bind at one end to laminin/nidogen complexes. Indeed we have observed protein tethers in sensory neurons cultured on highly purified laminin-111 (data not shown), a substrate that fully supports the RA-mechanosensitive current (Figure 2). We cannot at the moment say whether the tether we have identified morphologically is a single protein or a multimeric complex like the hair cell tip link (Ahmed *et al*, 2006; Kazmierczak *et al*, 2007). Nevertheless, our quantitative TEM data indicates that the filamentous objects >75 nm are remarkably homogenous in terms of size (mean 99 ± 18 nm standard deviation, from all measurements made) despite being measured in ultrathin sections in which its orientation is necessarily variable. Assuming that the protein tether that we have identified anatomically is necessary for activation of the RA-mechanosenitive then we can conclude that this tether does not share any biochemical characteristics with tip-link proteins in hair cells. The protein tether identified here is laminin binding, subtilisin-sensitive and Ca^{2+}-ion-independent, all features not shared by the hair cell tip link. Importantly, the extracellular part of the protein we have identified must contain at least one blisterase/furin consensus site, both cadherin-23 and protocadherin-15 do not contain such a consensus site, ascertained using the ELM server at http://elm.eu.org/ (Puntervoll *et al*, 2003). The requirement that at least one component of the protein tether identified here must contain a blisterase/furin site should considerably help in the identification of its molecular nature. Furin is a very well-characterized membrane-associated proprotein convertase that processes many membrane proteins, including epithelial sodium channels (Scamuffa *et al*, 2006; Hughey *et al*, 2007). The fact that the tether we have identified here is sensitive to soluble furin applied outside the cell, strongly suggests that this protein is protected from proteolytic processing during its normal biosynthesis in neurons. We have shown that the tether is synthesized by sensory neurons and that its presence is likely required for normal gating of the RA-mechanosensitive current. We speculate that the tether demonstrated here functions to channel force to the transduction channel or to the immediate lipid environment surrounding the channel. In this way the tether may have a function in touch receptors similar as that the tip link has in the hair cell. The identification of an extracellular protein tether necessary for mechanotransduction in vertebrate touch receptors opens up a unique opportunity to unravel the molecular components necessary for the gating of touch-relevant mechanotransduction channels.

Materials and methods

Whole-cell patch-clamp recordings from isolated DRG neurons

Whole-cell recordings were made from DRG neurons using fire-polished glass electrodes with a resistance of 3–5 MΩ. The extracellular solution contained (in mM) 140 NaCl, 1 $MgCl_2$, 2 $CaCl_2$, 4 KCl, 4 glucose, 10 HEPES, pH 7.4, and the electrodes were filled with a solution containing (in mM) 122 KCl, 10 NaCI, 1 $MgCl_2$, 1 EGTA, 10 HEPES, pH7.3. For most experiments, 0.1% Lucifer Yellow was included in the electrode. The cells were perfused with drug-containing solutions by moving an array of outlets in front of the patched cells (WAS02; Ditel, Prague). TTX was prepared in a final concentration of 1 μM in extracellular solution.

Observations were made using a Zeiss Axiovert 200 microscope equipped with a TILL imaging system, including the polychome V, a CCD camera and the imaging software TILLvisION. Membrane current and voltage were amplified and acquired using an EPC-10 amplifier sampled at 40 kHz; acquired traces were analysed using the Patchmaster and Fitmaster software (HEKA). For most experiments the membrane voltage was held at −60 mV with the voltage-clamp circuit.

Mechanical stimuli were applied using a heat-polished glass pipette (tip diameter 2–5 μm), driven by a MM3A Micromanipulator system (Kleindiek), positioned at an angle of 45 degrees to the surface of the dish. There are two different movements for the Nanomotor®: 'fine mode' and 'coarse mode'. Fine mode movement from any position is limited to about 740 nm in each direction from the *Z*-axis (calibrated by a Piezo actuator calibration device LL10PZT; LASERTEX). Coarse mode steps (one step about 750 nm) can be executed in any direction until the micromanipulator reaches its physical limits. The probe was positioned near the neurite or cell body, moved forward in steps of 200–750 nm for 500 ms and then withdrawn. If there was no response, the probe was moved forward by one step coarse mode; the same procedure was repeated until a mechanically activated inward current was recorded. The probe was moved at a speed of 1.4 μm ms^{-1} for the fine mode and 7.5 μm ms^{-1} for the coarse mode. For analysis of the kinetic properties of mechanically activated current, traces were fit with single exponential functions using the Fitmaster software (HEKA). Data are presented as mean ± s.e.m.

Electron microscopy

DRG or SCG neurons were isolated and cultivated on laminin-coated petriPERM dishes using standard culture conditions (Hu and Lewin, 2006) (petriPERM35; Vivascience AG, Germany). After 24 h, cells were washed twice with 0.1 M cacodylate buffer (Electron Microscopy Sciences, PA, USA), fixed in 2.5% glutaraldehyde for 4 h and stained with osmium tetroxide (Sigma-Aldrich Co. Ltd.) in the presence of ruthenium red (Fluka) to enhance the electron density of extracellular proteins (Hasko and Richardson, 1988). The fixed samples were dehydrated through a series of ethanol exchanges and infiltrated in a mixture of epoxy resin and propylene oxide (Polysciences Inc., Warrington, PA, USA) then embedded in epoxy resin. The embedded samples were randomly sectioned (50 nm thick) and then contrasted with uranyl acetate and lead citrate (Serva, Germany), and examined with a Zeiss 910 electron microscope. Digital micrographs were taken with a 1kx1k high-speed, slow-scan CCD camera (Proscan) and analysed with the iTEM software (Olympus Soft Imaging Solutions, Münster, Germany). To quantify electron-dense objects under different experimental conditions, microscopic fields were randomly photographed from at least 3–4 cultures in each group and the number and length of electron-dense objects that linked the neurite membrane to the laminin substrate were measured. The sum of the measured area of membrane contact was determined by the sum of the product of neurite contact zone width and the thickness of each ultrathin section. To generate the presentation of raw data as dot clouds, the length of each object was randomly plotted in two-dimensional space. To quantify the average interface distance between the neurite membrane and the laminin substrate, the ratio of interface area (nm^2) and neurite width along the contact zone (nm) was calculated from each electron micrograph.

Cell culture

The fibroblast cell line (mouse NIH 3T3 cells) was maintained in Dulbecco's modified Eagle's medium (DMEM), supplemented with 10% foetal bovine serum, penicillin, streptomycin and glutamine. Confluent cells were sub-cultured each week. Excess cells were irradiated as a suspension with 60 Gy (6000 rads) γ-irradiation. DRG neurons from adult mouse were prepared as described previously (Mannsfeldt *et al*, 1999; Stucky *et al*, 2002). No nerve growth factor or other neurotrophin was added to the medium. When co-cultured with 3T3 cells, DRG neurons were

plated on top of the 3T3 monolayer instead of on PLL/laminin substrate.

All the culture treatments were applied at least 16 h following plating after neurite outgrowth was established. DRG neurons were treated with CD29 (20 μg ml^{-1}, 90–270 min, 37°C), or PIPLC (25 U ml^{-1}, 120 min, 37°C) or BAPTA (5 mM, 30 min, 37°C). Immediately following these various treatments, neurons were prepared for whole-cell patch-clamp recordings and the presence or absence of mechanosensitive currents was measured (nominally between 0 and 3 h following treatment). Normally, the first recorded cells were obtained within the first 10 min following placement of the cells in the recording chamber.

Supplementary data

Supplementary data are available at *The EMBO Journal* Online (http://www.embojournal.org).

Acknowledgements

We thank the members of the Lewin laboratory for advice and comments on the paper. H Thränhardt and Anja Wegner provided excellent technical support. We are grateful to Bettina Erdmann, head of the MDC EM core facility, for help and advice. This work was supported by grant from the Deutsche Forschunsggemeinschaft (to GRL) and a von Humboldt fellowship to JH. Author contributions: JH conducted all electrophysiological experiments, LYC performed all the TEM work and MK provided purified laminin proteins. JH and LYC analysed the data. GRL and JH wrote the paper.

Conflict of interest

The authors declare that they have no conflict of interest.

References

Ahmed ZM, Goodyear R, Riazuddin S, Lagziel A, Legan PK, Behra M, Burgess SM, Lilley KS, Wilcox ER, Riazuddin S, Griffith AJ, Frolenkov GI, Belyantseva IA, Richardson GP, Friedman TB (2006) The tip-link antigen, a protein associated with the transduction complex of sensory hair cells, is protocadherin-15. *J Neurosci* **26:** 7022–7034

Assad JA, Shepherd GM, Corey DP (1991) Tip-link integrity and mechanical transduction in vertebrate hair cells. *Neuron* **7:** 985–994

Beurg M, Fettiplace R, Nam JH, Ricci AJ (2009) Localization of inner hair cell mechanotransducer channels using high-speed calcium imaging. *Nat Neurosci* **12:** 553–558

Bravo DA, Gleason JB, Sanchez RI, Roth RA, Fuller RS (1994) Accurate and efficient cleavage of the human insulin proreceptor by the human proprotein-processing protease furin. Characterization and kinetic parameters using the purified, secreted soluble protease expressed by a recombinant baculovirus. *J Biol Chem* **269:** 25830–25837

Chalfie M (2009) Neurosensory mechanotransduction. *Nat Rev Mol Cell Biol* **10:** 44–52

Cho H, Koo JY, Kim S, Park SP, Yang Y, Oh U (2006) A novel mechanosensitive channel identified in sensory neurons. *Eur J Neurosci* **23:** 2543–2550

Cho H, Shin J, Shin CY, Lee SY, Oh U (2002) Mechanosensitive ion channels in cultured sensory neurons of neonatal rats. *J Neurosci* **22:** 1238–1247

Chung YD, Zhu J, Han Y, Kernan MJ (2001) nompA encodes a PNS-specific, ZP domain protein required to connect mechanosensory dendrites to sensory structures. *Neuron* **29:** 415–428

Cueva JG, Mulholland A, Goodman MB (2007) Nanoscale organization of the MEC-4 DEG/ENaC sensory mechanotransduction channel in *Caenorhabditis elegans* touch receptor neurons. *J Neurosci* **27:** 14089–14098

Di Castro A, Drew LJ, Wood JN, Cesare P (2006) Modulation of sensory neuron mechanotransduction by PKC- and nerve growth factor-dependent pathways. *Proc Natl Acad Sci USA* **103:** 4699–4704

Drew LJ, Rohrer DK, Price MP, Blaver KE, Cockayne DA, Cesare P, Wood JN (2004) Acid-sensing ion channels ASIC2 and ASIC3 do not contribute to mechanically activated currents in mammalian sensory neurones. *J Physiol* **556:** 691–710

Drew LJ, Rugiero F, Cesare P, Gale JE, Abrahamsen B, Bowden S, Heinzmann S, Robinson M, Brust A, Colless B, Lewis RJ, Wood JN (2007) High-threshold mechanosensitive ion channels blocked by a novel conopeptide mediate pressure-evoked pain. *PLoS ONE* **2:** e515

Drew LJ, Wood JN, Cesare P (2002) Distinct mechanosensitive properties of capsaicin-sensitive and -insensitive sensory neurons. *J Neurosci* **22:** RC228

Emtage L, Gu G, Hartwieg E, Chalfie M (2004) Extracellular proteins organize the mechanosensory channel complex in *C. elegans* touch receptor neurons. *Neuron* **44:** 795–807

Fain GL (2003) *Sensory Transduction*. Sunderland, Massachusets: Sinauer Associates

Gillespie PG, Walker RG (2001) Molecular basis of mechanosensory transduction. *Nature* **413:** 194–202

Goodyear R, Richardson G (1999) The ankle-link antigen: an epitope sensitive to calcium chelation associated with the hair-cell surface and the calycal processes of photoreceptors. *J Neurosci* **19:** 3761–3772

Goodyear RJ, Richardson GP (2003) A novel antigen sensitive to calcium chelation that is associated with the tip links and kinocilial links of sensory hair bundles. *J Neurosci* **23:** 4878–4887

Gu G, Caldwell GA, Chalfie M (1996) Genetic interactions affecting touch sensitivity in *Caenorhabditis elegans*. *Proc Natl Acad Sci USA* **93:** 6577–6582

Guharay F, Sachs F (1984) Stretch-activated single ion channel currents in tissue-cultured embryonic chick skeletal muscle. *J Physiol* **352:** 685–701

Hasko JA, Richardson GP (1988) The ultrastructural organization and properties of the mouse tectorial membrane matrix. *Hear Res* **35:** 21–38

Hoger U, Torkkeli PH, Seyfarth EA, French AS (1997) Ionic selectivity of mechanically activated channels in spider mechanoreceptor neurons. *J Neurophysiol* **78:** 2079–2085

Honore E (2007) The neuronal background K2P channels: focus on TREK1. *Nat Rev Neurosci* **8:** 251–261

Hu J, Lewin GR (2006) Mechanosensitive currents in the neurites of cultured mouse sensory neurones. *J Physiol* **577:** 815–828

Hu J, Milenkovic N, Lewin GR (2006) The high threshold mechanotransducer: a status report. *Pain* **120:** 3–7

Hughey RP, Carattino MD, Kleyman TR (2007) Role of proteolysis in the activation of epithelial sodium channels. *Curr Opin Nephrol Hypertens* **16:** 444–450

Jasti J, Furukawa H, Gonzales EB, Gouaux E (2007) Structure of acid-sensing ion channel 1 at 1.9 A resolution and low pH. *Nature* **449:** 316–323

Kazmierczak P, Sakaguchi H, Tokita J, Wilson-Kubalek EM, Milligan RA, Muller U, Kachar B (2007) Cadherin 23 and protocadherin 15 interact to form tip-link filaments in sensory hair cells. *Nature* **449:** 87–91

Kellenberger S, Schild L (2002) Epithelial sodium channel/degenerin family of ion channels: a variety of functions for a shared structure. *Physiol Rev* **82:** 735–767

Khalsa PS, Ge W, Zia Uddin M, Hadjiargyrou M (2004) Integrin alpha2beta1 affects mechano-transduction in slowly and rapidly adapting cutaneous mechanoreceptors in rat hairy skin. *Neuroscience* **129:** 447–459

Kinoshita T, Fujita M, Maeda Y (2008) Biosynthesis, remodelling and functions of mammalian GPI-anchored proteins: recent progress. *J Biochem* **144:** 287–294

Koerber HR, Druzinsky RE, Mendell LM (1988) Properties of somata of spinal dorsal root ganglion cells differ according to peripheral receptor innervated. *J Neurophysiol* **60:** 1584–1596

Kung C (2005) A possible unifying principle for mechanosensation. *Nature* **436:** 647–654

Lane JW, McBride Jr DW., Hamill OP (1991) Amiloride block of the mechanosensitive cation channel in *Xenopus* oocytes. *J Physiol* **441:** 347–366

Lechner SG, Frenzel H, Wang R, Lewin GR (2009) Developmental waves of mechanosensitivity acquisition in sensory neuron subtypes during embryonic development. *EMBO J* **28:** 1479–1491

Lechner SG, Lewin GR (2009) Peripheral sensitisation of nociceptors via G-protein-dependent potentiation of mechanotransduction currents. *J Physiol* **587:** 3493–3503

Lewin GR, Moshourab R (2004) Mechanosensation and pain. *J Neurobiol* **61:** 30–44

Lumpkin EA, Hudspeth AJ (1995) Detection of Ca2 + entry through mechanosensitive channels localizes the site of mechano-electrical transduction in hair cells. *Proc Natl Acad Sci USA* **92:** 10297–10301

Mannsfeldt AG, Carroll P, Stucky CL, Lewin GR (1999) Stomatin, a MEC-2 like protein, is expressed by mammalian sensory neurons. *Mol Cell Neurosci* **13:** 391–404

Martinez-Salgado C, Benckendorff AG, Chiang LY, Wang R, Milenkovic N, Wetzel C, Hu J, Stucky CL, Parra MG, Mohandas N, Lewin GR (2007) Stomatin and sensory neuron mechanotransduction. *J Neurophysiol* **98:** 3802–3808

McCarter GC, Levine JD (2006) Ionic basis of a mechanotransduction current in adult rat dorsal root ganglion neurons. *Mol Pain* **2:** 28

McCarter GC, Reichling DB, Levine JD (1999) Mechanical transduction by rat dorsal root ganglion neurons *in vitro*. *Neurosci Lett* **273:** 179–182

Mendrick DL, Kelly DM (1993) Temporal expression of VLA-2 and modulation of its ligand specificity by rat glomerular epithelial cells *in vitro*. *Lab Invest* **69:** 690–702

Milenkovic N, Wetzel C, Moshourab R, Lewin GR (2008) Speed and temperature dependences of mechanotransduction in afferent fibers recorded from the mouse saphenous nerve. *J Neurophysiol* **100:** 2771–2783

Morris CE, Horn R (1991) Failure to elicit neuronal macroscopic mechanosensitive currents anticipated by single-channel studies. *Science* **251:** 1246–1249

Nakayama K (1997) Furin: a mammalian subtilisin/Kex2p-like endoprotease involved in processing of a wide variety of precursor proteins. *Biochem J* **327**(Pt 3)**:** 625–635

O'Hagan R, Chalfie M, Goodman MB (2005) The MEC-4 DEG/ENaC channel of *Caenorhabditis elegans* touch receptor neurons transduces mechanical signals. *Nat Neurosci* **8:** 43–50

Osborne MP, Comis SD (1990) Action of elastase, collagenase and other enzymes upon linkages between stereocilia in the guinea-pig cochlea. *Acta Otolaryngol* **110:** 37–45

Paulsson M, Aumailley M, Deutzmann R, Timpl R, Beck K, Engel J (1987) Laminin–nidogen complex. Extraction with chelating agents and structural characterization. *Eur J Biochem* **166:** 11–19

Poole CB, Jin J, McReynolds LA (2003) Cloning and biochemical characterization of blisterase, a subtilisin-like convertase from the filarial parasite, *Onchocerca volvulus*. *J Biol Chem* **278:** 36183–36190

Puntervoll P, Linding R, Gemund C, Chabanis-Davidson S, Mattingsdal M, Cameron S, Martin DM, Ausiello G, Brannetti B, Costantini A, Ferre F, Maselli V, Via A, Cesareni G, Diella F, Superti-Furga G, Wyrwicz L, Ramu C, McGuigan C, Gudavalli R *et al* (2003) ELM server: a new resource for investigating short functional sites in modular eukaryotic proteins. *Nucleic Acids Res* **31:** 3625–3630

Scamuffa N, Calvo F, Chretien M, Seidah NG, Khatib AM (2006) Proprotein convertases: lessons from knockouts. *FASEB J* **20:** 1954–1963

Sharif-Naeini R, Folgering JH, Bichet D, Duprat F, Lauritzen I, Arhatte M, Jodar M, Dedman A, Chatelain FC, Schulte U, Retailleau K, Loufrani L, Patel A, Sachs F, Delmas P, Peters DJ, Honore E (2009) Polycystin-1 and -2 dosage regulates pressure sensing. *Cell* **139:** 587–596

Siemens J, Lillo C, Dumont RA, Reynolds A, Williams DS, Gillespie PG, Muller U (2004) Cadherin 23 is a component of the tip link in hair-cell stereocilia. *Nature* **428:** 950–955

Sollner C, Rauch GJ, Siemens J, Geisler R, Schuster SC, Muller U, Nicolson T (2004) Mutations in cadherin 23 affect tip links in zebrafish sensory hair cells. *Nature* **428:** 955–959

Spinelli KJ, Gillespie PG (2009) Bottoms up: transduction channels at tip link bases. *Nat Neurosci* **12:** 529–530

Stucky CL, Rossi J, Airaksinen MS, Lewin GR (2002) GFR alpha2/neurturin signalling regulates noxious heat transduction in isolectin B4-binding mouse sensory neurons. *J Physiol* **545:** 43–50

Sukharev SI, Blount P, Martinac B, Blattner FR, Kung C (1994) A large-conductance mechanosensitive channel in *E. coli* encoded by mscL alone. *Nature* **368:** 265–268

Sukharev SI, Martinac B, Arshavsky VY, Kung C (1993) Two types of mechanosensitive channels in the *Escherichia coli* cell envelope: solubilization and functional reconstitution. *Biophys J* **65:** 177–183

Swerup C, Rydqvist B, Ottoson D (1983) Time characteristics and potential dependence of early and late adaptation in the crustacean stretch receptor. *Acta Physiol Scand* **119:** 91–99

Tomaselli KJ, Doherty P, Emmett CJ, Damsky CH, Walsh FS, Reichardt LF (1993) Expression of beta 1 integrins in sensory neurons of the dorsal root ganglion and their functions in neurite outgrowth on two laminin isoforms. *J Neurosci* **13:** 4880–4888

Vallet V, Chraibi A, Gaeggeler HP, Horisberger JD, Rossier BC (1997) An epithelial serine protease activates the amiloride-sensitive sodium channel. *Nature* **389:** 607–610

Wetzel C, Hu J, Riethmacher D, Benckendorff A, Harder L, Eilers A, Moshourab R, Kozlenkov A, Labuz D, Caspani O, Erdmann B, Machelska H, Heppenstall PA, Lewin GR (2007) A stomatin-domain protein essential for touch sensation in the mouse. *Nature* **445:** 206–209

Zhao Y, Yamoah EN, Gillespie PG (1996) Regeneration of broken tip links and restoration of mechanical transduction in hair cells. *Proc Natl Acad Sci USA* **93:** 15469–15474